International Journal of Heat and Mass Transfer 127 (2018) 1084–1094

Contents lists available at ScienceDirect

International Journal of Heat and Mass Transfer

journal homepage: www.elsevier.com/locate/ijhmt

Fusion zone geometries, cooling rates and solidification parameters during wire arc additive manufacturing

W. Ou [a,b], T. Mukherjee [a], G.L. Knapp [a], Y. Wei [b], T. DebRoy [a,*]

[a] Department of Materials Science and Engineering, The Pennsylvania State University, University Park, PA 16802, USA
[b] Department of Material Science and Technology, Nanjing University of Aeronautics and Astronautics, Jiangsu 210016, China

ARTICLE INFO

Article history:
Received 14 May 2018
Received in revised form 17 July 2018
Accepted 23 August 2018

Keywords:
Wire arc additive manufacturing
Heat transfer and fluid flow
Cooling rates
Solidification parameters
H13 tool steel

ABSTRACT

Structure, properties and serviceability of components made by wire arc additive manufacturing (WAAM) depend on the process parameters such as arc power, travel speed, wire diameter and wire feed rate. However, the selection of appropriate processing conditions to fabricate defect free and structurally sound components by trial and error is expensive and time consuming. Here we develop, test and utilize a three-dimensional heat transfer and fluid flow model of WAAM to calculate temperature and velocity fields, deposit shape and size, cooling rates and solidification parameters. The calculated fusion zone geometries and cooling rates for various arc power and travel speed and thermal cycles considering convective flow of molten metal agreed well with the corresponding experimental data for H13 tool steel deposits. It was found that convection is the main mechanism of heat transfer inside the molten pool. Faster travel speed enhanced the cooling rate but reduced the ratio of temperature gradient to solidification growth rate indicating increased instability of plane front solidification of components. Higher deposition rates could be achieved by increasing the heat input, using thicker wires and rapid wire feeding.

1. Introduction

Wire arc additive manufacturing (WAAM) is developed from arc welding and suitable for making large components because of high deposition rates, low equipment and feedstock costs [1]. WAAM involves melting of wire by the arc, transfer of molten metal droplets to a molten pool, convective flow of liquid metal inside the molten pool driven by surface tension gradient [2–4], deformation of the molten pool surface by arc pressure and solidification of the molten pool [2,3]. These physical phenomena govern the temperature and velocity distributions, deposit shape and size, and the structure and properties of the components. In addition, transient and spatially non-uniform temperature field results in residual stresses and distortion [5–8]. Therefore, fabrication of a structurally sound and defect free WAAM component requires precise control of the process by appropriate selection of the process variables such as arc power, travel speed, wire diameter and wire feed rate. However, selection of these variables by trial and error is expensive, time consuming and provides no guarantee of achieving the desired structure and properties. A recourse is to develop, test and utilize a mathematical framework that can serve as a basis for selecting appropriate process conditions based on scientific principles.

WAAM has already been successfully applied for making components of steels [7,9,10], aluminum alloys [11,12], titanium alloys [13,14] and nickel alloys [15] and several attempts have been made to model the process. Analytical models have been used to predict build geometry [16,17] and surface topology [18]. However, these models are based on empirical formulae and ignore the heat and mass transfer during the process. Heat conduction models have also been used to calculate temperature distribution [19,20], temperature gradient [21] and residual stresses [19]. However, these models neglect the convective flow of liquid metal inside the molten pool that often dominates the heat transfer mechanism inside the molten pool. Manvatkar et al. [22] and Arrizubieta et al. [23] noted that calculations neglecting the convective heat transfer significantly overestimate the peak temperature and cooling rates. Svensson et al. [24] mentioned that the heat conduction calculations are inadequate to accurately calculate the cooling rates. Volume of fluid (VOF) based numerical models used by Silwal et al. [25] consider the molten metal convection and have been used to predict the deposit geometry. However, these models are computationally expensive and have not been used to estimate essential metallurgical variables such as temperature gradient, cooling rates and solidification parameters. What is needed and currently not available is a well-tested comprehensive phenomenological

* Corresponding author.
E-mail address: debroy@psu.edu (T. DebRoy).

https://doi.org/10.1016/j.ijheatmasstransfer.2018.08.111
0017-9310/

model of WAAM capable of calculating the essential metallurgical variables for different process variables.

Here we develop, test and use a three-dimensional heat transfer and fluid flow model of wire arc additive manufacturing to calculate the temperature and velocity fields, deposit shape and size, cooling rates and solidification parameters for a single-track deposit. Experiments are conducted by depositing H13 tool steel at different arc powers and travel speeds to validate the model. The variations of fusion zone geometry with power and travel speed are compared with the corresponding experimental results. Calculated temperature variation with time is also tested against independent experimental data. After validation, the model is used to quantitatively study the effects of a wide variety of process variables such as arc power, travel speed, wire feed rate and wire diameter on different metallurgical variables.

2. Theoretical model

2.1. Assumptions

The following simplifying assumptions are made to make the numerical calculations involving heat and fluid flow, droplet transfer and molten pool surface geometry tractable.

(1) The liquid metal is assumed to be a Newtonian fluid and its viscosity depends on temperature and pressure [26]. The Boussinesq approximation is used for the calculation of buoyancy driven flow [6].
(2) Effective thermal conductivity and viscosity of the liquid metal are enhanced to account for turbulent convection effects [27]. No separate turbulence models are used to estimate turbulent components of transport properties.
(3) Because the arc current in the WAAM process is higher than 100 A, metal transfer mode is assumed to be globular-type [28]. Due to difficulties with the measurement, droplet temperature is calculated based on net heat balance [29]. The droplet velocity is calculated considering arc plasma effect using the formula provided by Kumar and Bhaduri [30].

2.2. Solution domain

The three-dimensional solution domain for a single-track deposit is shown in Fig. 1. Calculations are done in the Cartesian coordinate system, which is attached to the heat source. In other words, the arc source and the molten pool are stationary in space, and the substrate material enters and leaves the computational domain at the scanning speed. Half of the solution domain is considered in the calculations by taking advantage of symmetry. Droplets impinge on the molten pool to form a deposit, and their sensible heat is considered as a volumetric heat source for the heat transfer calculations [29]. The surface of the deposit is assumed to be flat during the calculation of the temperature and velocity fields. After the calculation, the free surface profile of the deposit is estimated by minimizing the total surface energy on the top surface of the deposit [31]. Finally, the grids are adjusted to fit the surface profile, and the temperature and velocity fields are then reassigned in the fitted grid system.

2.3. Governing equations

The heat transfer and fluid flow model solves the equations of conservation of mass, momentum and energy in three components along the x, y, and z directions [32,33].

$$\frac{\partial(\rho u_i)}{\partial x_i} = 0 \tag{1}$$

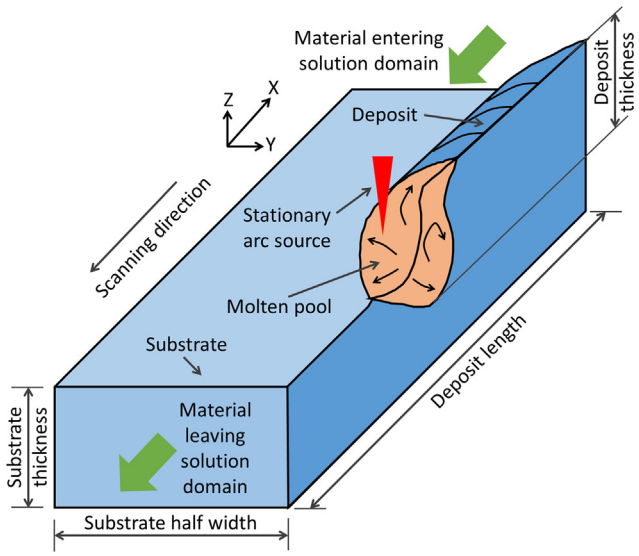

Fig. 1. Schematic of the solution domain consisting of molten pool, substrate and deposit. The dimensions are given in Table 2. Scanning direction is along negative X-axis. Half of the solution domain is used because of the symmetry with respect to XZ-plane.

$$\frac{\partial(\rho u_j u_i)}{\partial x_i} = \frac{\partial}{\partial x_i}\left(\mu \frac{\partial u_j}{\partial x_i}\right) + S_j \tag{2}$$

$$\frac{\partial(\rho u_i h)}{\partial x_i} = \frac{\partial}{\partial x_i}\left(\frac{k}{C_P}\frac{\partial h}{\partial x_i}\right) - \rho U_S \frac{\partial h}{\partial x_i} + S_L + S_V \tag{3}$$

where ρ is the density, u_i and u_j are the velocity components along the i- and j-directions, respectively, and x_i is the distance along the i-direction, μ is the effective viscosity, and S_j is a source term for the momentum equation (2) including buoyancy force, the motion of the heat source, electromagnetic force and frictional dissipation in the mushy zone. These source terms were described in detail by Zhang et al. [31] and Mundra et al. [34]. The symbol h is the sensible heat, C_P is the specific heat, k is the thermal conductivity, U_S is the scanning speed, S_L is the source term that accounts for latent heat and S_V is the source term for the additional heat from metal droplets. The source term S_V is calculated assuming that the heat energy from the metal droplets is distributed uniformly in a cylindrical cavity inside the work piece [29,34,35]. Detail derivation of the source term S_V is presented in Appendix A. The thermophysical properties of the alloys are provided in Table 1 [36,37].

Table 1
Thermo-physical properties of AISI 1040 steel, H13 steel, and ER70S-6 steel [36,37]. Arc efficiencies are estimated following Haelsig et al. [44].

Properties	AISI 1040	H13	ER70S-6
Liquidus temperature (K)	1745	1585	1712
Solidus temperature (K)	1800	1725	1766
Thermal conductivity of solid (W/mK)	25.3	30.4	33.0
Thermal conductivity of liquid (W/mK)	34.0	31.0	35.4
Enhanced thermal conductivity of liquid, (W/mK)	253.0	304.0	283.3
Specific heat of solid (J/kg K)	696.3	734.3	701.3
Specific heat of liquid (J/kg K)	700.4	823.4	902.5
Density (kg/m^3)	7290	7800	7700
Viscosity (kg/m s)	6.4×10^{-3}	5.7×10^{-3}	5.7×10^{-3}
Enhanced viscosity, (kg/m s)	29.6×10^{-3}	105×10^{-3}	26.4×10^{-3}
$d\gamma/dT$ (N/m K)	-0.40×10^{-3}	-0.43×10^{-3}	-0.41×10^{-3}
Arc efficiency	0.67	0.67	0.82